J. Appl. Biol. Sci., 20 (1): 24-33, January 2026
https://dx.doi.org/10.71336/jabs.1501
RESEARCH ARTICLE

Journal of Applied Biological Sciences
EISSN: 2146-0108; License: CC BY 4.0
JABS Anatolia Academy of Sciences Open Access

In silico analysis of LDLR isoform gene for the identification of natural inhibitors against familial hypercholesterolemia

Sadia Ali[1*], Esha Shahid[1], Aysha Shafique[1], Rabia Pervaiz[1], Ayesha[1], Amad Ul Hassan[1], Bilal Ilyas[1], Zain Ul Abidin[1], Tanzeel Ur Rehman[1], Zainab Aqsa[2], Ayesha Nawaz[3], Areeba Younas[4], and Maham Rafique[4]

[1]*University of Central Punjab Lahore, Faculty of Science and Technology, Department of Biotechnology, Lahore, Pakistan*

[2]*University of Central Punjab Lahore, Faculty of Science and Technology, Department of Food Science and Technology, Lahore, Pakistan*

[3]*University of Central Punjab Lahore, Faculty of Science and Technology, Department of Microbiology, Lahore, Pakistan*

[4]*University of Central Punjab Lahore, Faculty of Science and Technology, Department of Zoology, Lahore, Pakistan*

*Correspondence:
Sadia Ali
Email: Sadiashah765@gmail.com

Received: May 21, 2025
Revised: September 9, 2025
Accepted: January 07, 2026

ABSTRACT: Familial hypercholesterolemia (FH) is a genetic disorder characterized by elevated low-density lipoprotein cholesterol (LDL-C), increasing the risk of premature cardiovascular disease. Loss-of-function mutations in the LDL receptor (LDLR) gene are the primary cause, reducing receptor-mediated LDL clearance. Current therapies, including statins, ezetimibe, and PCSK9 inhibitors, aim to enhance LDLR function but may have side effects or limited efficacy, highlighting the need for alternative strategies. This study employed an in silico approach to identify natural phytochemicals capable of modulating LDLR. Five compounds guggulsterone, curcumin, β-sitosterol, oleuropein, and resveratrol were evaluated for binding affinity, pharmacokinetics, and toxicity. LDLR secondary and tertiary structures were predicted using GOR IV, PSIPRED, and AlphaFold, with binding sites identified via DeepSite. Molecular docking using PyRx and CB-Dock2 showed guggulsterone as the top candidate, exhibiting a binding affinity of -9.4 kcal/mol and stable hydrogen bond and hydrophobic interactions with key residues. ADMET analysis indicated high gastrointestinal absorption, Lipinski rule compliance, and minimal organ-specific toxicity, although blood-brain barrier permeability was predicted. These findings suggest that guggulsterone may stabilize LDLR or influence receptor regulation, providing a potential natural therapeutic approach for FH. Further in vitro and in vivo studies are warranted to confirm efficacy and elucidate mechanisms.

KEYWORDS: Familial Hypercholesterolemia, Low density lipoprotein, Guggulsterone, Molecular docking, Statins, Toxicity

INTRODUCTION

Familial hypercholesterolemia (FH) is an inherited metabolic disorder characterized by persistently elevated levels of low-density lipoprotein cholesterol (LDL-C), which significantly increases the risk of premature cardiovascular disease [1] . It is one of the most common monogenic lipid disorders worldwide, affecting approximately 1 in 250 individuals, yet it remains largely underdiagnosed. The clinical manifestations of FH include markedly raised LDL-C levels, early-onset atherosclerotic cardiovascular disease, tendon xanthomas, and corneal arcus, particularly in untreated individuals [2].

At the molecular level, FH most frequently arises from pathogenic variants in genes involved in LDL metabolism, particularly the low-density lipoprotein receptor (LDLR), apolipoprotein B (APOB), and proprotein convertase subtilisin/kexin type 9 (PCSK9) [3]. Among these, loss-of-function mutations in LDLR represent the predominant cause. LDLR plays a critical role in mediating the hepatic uptake and clearance of circulating LDL particles. Impaired LDLR expression or function leads to reduced receptor-mediated LDL clearance, resulting in elevated plasma LDL-C concentrations and accelerated atherosclerosis [4].

Current therapeutic strategies for FH aim to reduce circulating LDL-C levels primarily by enhancing LDLR availability and function. Statins, ezetimibe, and PCSK9 inhibitors are commonly used to achieve this goal by upregulating LDLR expression or preventing LDLR degradation. Despite their effectiveness, these therapies may be associated with adverse effects, variable patient response, high cost, or limited efficacy in severe forms of FH, highlighting the need for alternative or complementary therapeutic approaches [5].

In recent years, in silico drug discovery approaches have emerged as valuable tools for identifying novel bioactive compounds with potential therapeutic relevance. Computational analysis allows rapid screening of small

How to cite this article: Ali S., Shahid E., Shafique A., Pervaiz R., Ayesha, Hassan A.U., Ilyas B., Abidin Z.U., Rehman T.U., Aqsa Z., Nawaz A., Younas A., and Rafique M. (2026). In silico analysis of LDLR isoform gene for the identification of natural inhibitors against familial hypercholesterolemia. *Journal of Applied Biological Sciences*, 20 (1): 24-33. https://dx.doi.org/10.71336/jabs.1501

molecules for their ability to interact with disease-related proteins, providing mechanistic insights prior to experimental validation. Natural phytochemicals, in particular, have gained attention due to their structural diversity, biological activity, and favorable safety profiles.

The present study employs an in silico strategy to analyze the structural features of the LDLR protein and to identify natural phytochemical compounds capable of binding to LDLR. Rather than proposing direct inhibition of LDLR activity, this work focuses on identifying compounds that may interact with LDLR in a manner relevant to receptor modulation, stabilization, or regulation. Such interactions may have implications for preserving LDLR function or influencing pathways involved in receptor turnover, including PCSK9-mediated degradation. The findings of this study provide a computational foundation for further experimental investigation into phytochemical-based therapeutic strategies for familial hypercholesterolemia.

MATERIALS AND METHODS

Sequence Retrieval of target protein

The amino acid sequence of the human low-density lipoprotein receptor (LDLR) protein (accession number XP_054176989.1) was retrieved from the National Center for Biotechnology Information (NCBI) https://www.ncbi.nlm.nih.gov/ [6] protein database. NCBI is a publicly accessible resource that curates and provides integrated biological sequence data for genomic and proteomic research.

Prediction of protein secondary structure

The secondary structure of the LDLR protein was predicted using the GOR IV server https://npsa-prabi.ibcp.fr/cgi-bin/npsa_automat.pl?page=/NPSA/npsa_gor4.html, which estimated the distribution of α-helices, β-strands, and random coils based on amino acid propensities. PSIPRED was subsequently employed to analyze the protein topology, identifying extracellular, transmembrane, and cytoplasmic regions by using position-specific scoring matrices derived from multiple sequence alignments [7].

Tertiary structure prediction and validation

The three-dimensional structure of the low-density lipoprotein receptor (LDLR) was obtained from the AlphaFold Protein Structure Database (https://alphafold.ebi.ac.uk/ accessed on 2 March 2024), which provides Artificial Intelligence-assisted predictions of protein structures. Structural quality was assessed using PROCHECK based on Ramachandran plot analysis [8].

Physiochemical Properties Analysis

Expasy ProtParam tool https://web.expasy.org/protparam/ utilized for physicochemical properties prediction of protein sequences, including amino acid composition, extinction coefficient, isoelectric point (pI), and atomic composition [9].

String Analysis and binding site prediction

Protein-protein interactions were analyzed using the STRING database (https://string-db.org/) [10]. DeepSite is a deep neural network-based tool designed to identify and modify protein binding sites. DeepSite is freely accessible online (https://playmolecule.org/deepsite/ ; accessed on 2 March 2014) [11].

Retrieval of natural compounds

Five phytochemical compounds curcumin, betasitosterol, guggulsterone, oleuropein, and resveratrol were selected as ligands and retrieved from the PubChem database https://pubchem.ncbi.nlm.nih.gov/ . These compounds were chosen based on their reported antioxidant and lipid-lowering properties, as well as prior evidence of potential beneficial effects on cardiovascular health. Table 1 presents the PubChem compound IDs, molecular weights, and chemical formula of the selected phytochemicals used in this study [12].

Table 1. PubChem IDs and basic chemical properties of the selected phytochemicals

Phytochemicals	PubChem CIDs	Molecular Weight	Chemical formula
Guggulsterone	6450278	312.4g/mol	$C_{21}H_{28}O_2$
Oleuropein	5281544	540.5g/mol	$C_{25}H_{32}O_{13}$
Curcumin	969516	368.4g/mol	$C_{21}H_{20}O_6$
Resveratrol	4445154	228.24g/mol	$C_{14}H_{12}O_3$
Betasitosterol	222284	414.7g/mol	$C_{29}H_{50}O$

Virtual Screening of natural compounds

Virtual screening of all selected ligands was performed using PyRx, an offline molecular docking and virtual screening platform. The three-dimensional structures of the ligands were imported into PyRx in SDF or PDB format and converted into PDBQT format, which contains information on atom types, torsional flexibility, and partial charges required for docking. Prior to docking, ligands were prepared by the addition of hydrogen atoms, optimization of protonation states, and generation of low-energy conformers to account for possible tautomeric forms, followed by energy minimization using the built-in Universal Force Field (UFF)

to reduce steric clashes and optimize molecular geometries. The LDLR protein was prepared by removing water molecules, maintaining disulfide bonds, and preserving glycosylation sites, with polar hydrogens added where necessary. Docking simulations were carried out using the AutoDock Vina engine integrated into PyRx, employing a grid box centered at X = 0, Y = 5, and Z = −3, with dimensions of 21 × 21 × 29 Å along the X, Y, and Z axes, respectively. An exhaustiveness value of 8 was used to ensure adequate sampling of ligand conformations within the binding region [13].

Molecular docking and interaction analysis

The docking results obtained from PyRx were further validated using CB-Dock2 http://183.56.231.194:8001/cb-dock2/index.php , which facilitates docking of ligands to protein binding cavities by incorporating cavity detection, docking, and homologous template fitting. Detailed interaction analysis was conducted using Discovery Studio, which allowed identification of the active residues of LDLR involved in ligand binding and characterization of the different types of interactions, including hydrogen bonds, hydrophobic contacts, and van der Waals forces. This combined approach provided a comprehensive understanding of ligand-protein interactions and supported the selection of the most promising phytochemical candidate [14] [15].

ADMET Analysis and Toxicity prediction

The SwissADME tool http://www.swissadme.ch/ was utilized to perform ADMET (Absorption, Distribution, Metabolism, Excretion, and Toxicity) analysis on the drug candidates for pre-clinical evaluation. This computational platform predicted pharmacokinetic properties and assessed medicinal and drug-like characteristics. Drug-likeness was further evaluated using the Molinspiration Cheminformatics server (https://www.molinspiration.com). Additionally, toxicity analysis of the ligands was conducted using the ProTox II server https://tox-new.charite.de/protox_II/index.php?site=home [16] [17].

RESULTS

Prediction of protein secondary structure

The secondary structure of the LDLR protein was predicted using the GOR IV server, which identified the distribution of α-helices, β-strands, and random coils, as illustrated in Figure 1. The analysis revealed that α-helices comprised 75 residues (8.99%), extended β-strands accounted for 237 residues (28.42%), and random coils represented the dominant structural component with 522 residues (62.59%) of the total sequence. Further structural topology analysis using PSIPRED indicated that the majority of the LDLR protein is localized in the extracellular region, encompassing amino acid residues 1–761. The transmembrane helix was predicted to span residues 762–780, while the cytoplasmic domain was assigned to residues 781–834, as depicted in Figure 2.

Prediction and validation of tertiary structure

Tertiary structure of the low-density lipoprotein receptor (LDLR) protein was obtained from alphaFold, as shown in Figure 3. Then structure was verified using the PROCHECK Ramachandran Plot. The analysis revealed that 90.1% of residues are situated in the most favored regions, 9.00% in additional allowed regions, 0.1% in generously allowed regions, and 0.8% in disallowed regions, as illustrated in Figure 4.

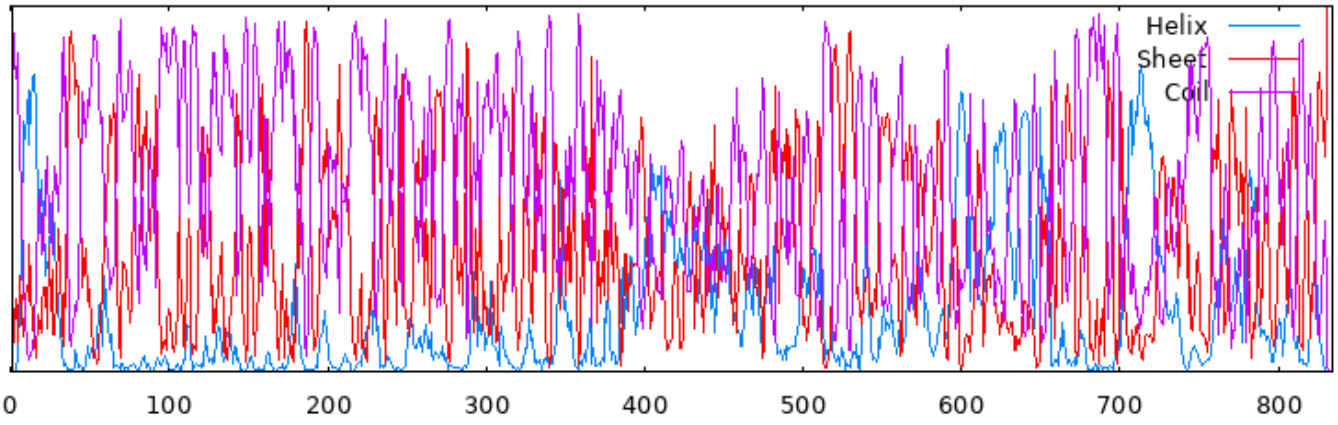

Figure 1. Secondary structure prediction of the LDLR protein showing α-helices, β-strands, and random coils.

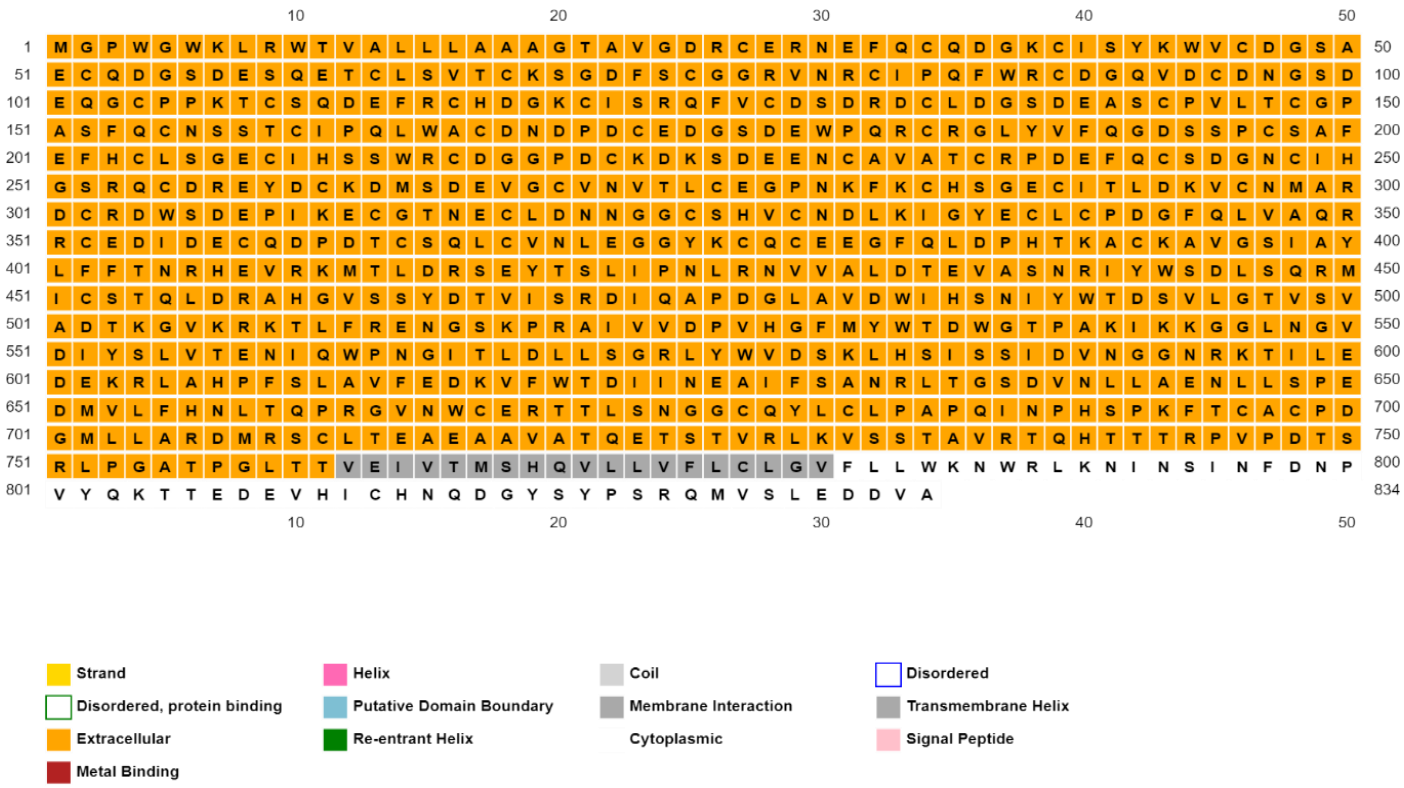

Figure 2. Topological organization of the LDLR protein indicating extracellular, transmembrane, and cytoplasmic regions.

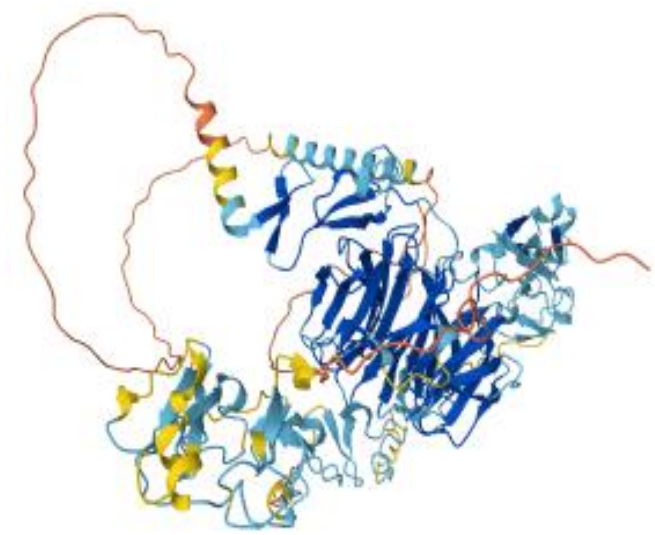

Figure 3. 3D Structure of Low-density lipoprotein receptor protein

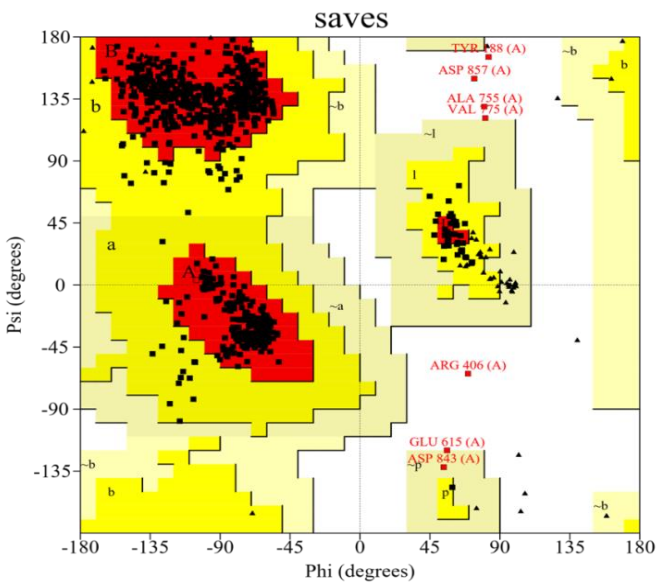

Figure 4. Ramachandran plot validating the 3d structure of LDLR protein

String Analysis and Binding Site Identification

The STRING database was employed to analyze protein-protein interactions involving the LDLR protein. The analysis revealed interactions with various proteins, represented by 11 nodes and 27 edges, as depicted in Figure 5. The DeepSite tool determined four distinct binding sites of protein. These sites are represented by orange-colored, net-like interwoven structures in Figure 6. The centers of these binding positions and their corresponding scores are detailed in Table 2.

Physiochemical properties analysis

The physicochemical characterization of the LDLR protein indicates that it is structurally stable and functionally well suited for interactions in an aqueous cellular environment. The instability index of 36.61 classifies the protein as stable, suggesting that it can maintain its structural integrity under physiological conditions. The aliphatic index of 69.28 reflects a moderate proportion of aliphatic amino acids, which contributes to reasonable thermal stability of the protein. The GRAVY value of −0.406 indicates an overall hydrophilic nature, implying good solubility and a tendency to interact favorably with water and other polar molecules rather than being strongly embedded within hydrophobic environments. The theoretical isoelectric point (pI) of 4.81 shows that the protein is acidic in nature and would carry a net negative charge at physiological pH, which may influence its binding behavior, solubility, and interactions with ligands or other biomolecules. The detailed physicochemical properties are summarized in Table 3.

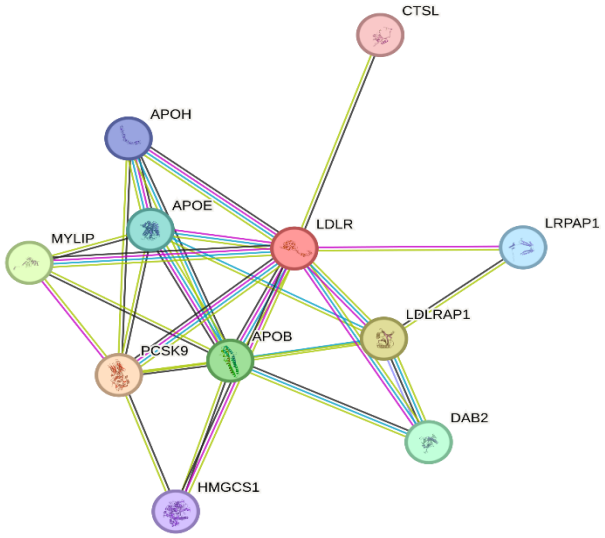

Figure 5. Interaction of LDLR protein with different proteins by STRING.

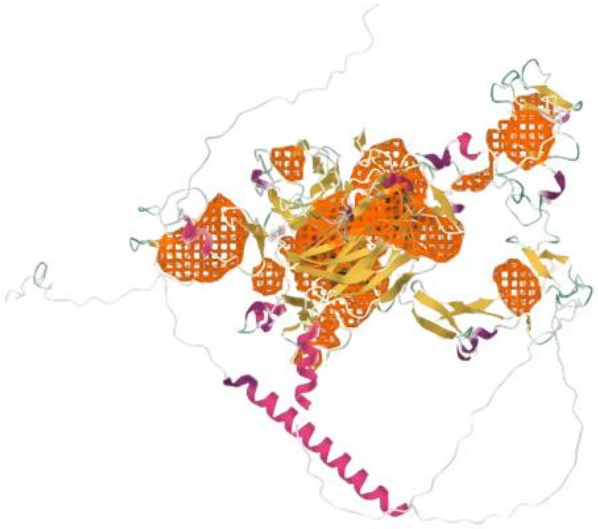

Figure 6. Binding sites of the protein predicted by DeepSite. The binding sites are represented by orange-colored, net-like interwoven structures.

Table 2. The scores and the centers of the binding sites.

Site No	Scores	Centers
1.	0.9992	[-8.720000267028809, -1.840000033378601, -1.9600000381469727]
2.	0.9903	[-32.720001220703125, -1.840000033378601, 58.040000915527344]
3.	0.9487	[35.279998779296875, 22.15999984741211, -7.960000038146973]
4.	0.9239	[1.2799999713897705, -1.840000033378601, -21.959999084472656]

Table 3. Physiochemical Characterization of LDLR Protein.

Parameters	Values
No. of Amino acids	834
Mol. weight	92745.94
Theoretical pI	4.81
No. of negatively charged residues	121
No. of positively charged residues	78
Formula	C3975H6166N1132O1285S74
No. of Atoms	12632
Instability Index	36.61 (Stable)
Estimated Half life	30 hrs (mammalian reticulocytes,in vitro). >20 hrs (yeast, in vivo). >10 hrs (E. coli, in vivo).
Aliphatic Index	69.28
GRAVY	-0.406 (Hydrophobic)

Virtual Screening of natural compounds

The virtual screening analysis evaluated the binding affinity of selected natural compounds against the LDLR protein using docking scores as the primary criterion. Among the screened ligands, guggulsterone showed the strongest binding potential, exhibiting the highest docking score of -9.7kcal/mol, indicating a high predicted affinity for the LDLR target. This was followed by oleuropein, which demonstrated a favorable docking score of -7.3kcal/mol, suggesting a stable interaction with the receptor. Curcumin also showed a comparable binding tendency, with a docking score of -7.1kcal/mol, placing it among the moderately strong binders. In contrast, resveratrol displayed a weaker interaction profile with a docking score of -6.1kcal/mol, while β-sitosterol exhibited the least binding affinity among the tested compounds, reflected by a docking score of -5.8kcal/mol. Overall, the docking results ranked the ligands in the order of guggulsterone > oleuropein > curcumin > resveratrol > β-sitosterol, highlighting guggulsterone as the most promising candidate for interaction with the LDLR protein based on binding energy values.

Molecular docking and interaction analysis

The docking results obtained from the initial virtual screening were further validated using the CB-Dock2 server to confirm the binding reliability and cavity preference of the selected ligand. Interaction analysis was subsequently carried out using BIOVIA Discovery Studio to elucidate the binding mode and key residue interactions. The two-dimensional interaction diagram illustrates the binding conformation of guggulsterone within the active site of the target protein (Figure 7 and 8). As depicted in Figure 7, guggulsterone exhibits a stable binding orientation supported by multiple non-covalent interactions. A conventional hydrogen bond was observed between the oxygen atom of guggulsterone and Isoleucine (ILE A:566), indicating a strong polar interaction that contributes significantly to ligand stabilization within the binding pocket. In addition to hydrogen bonding, alkyl (hydrophobic) interactions were identified between guggulsterone and Proline (PRO A:526) as well as Valine (VAL A:653), which enhance hydrophobic complementarity and binding affinity.

Furthermore, the ligand is surrounded by several residues forming van der Waals interactions, including Trp A:483, Gln A:660, Thr A:659, Thr A:567, Met A:652, Leu A:654, Leu A:611, Gly A:565, Ser A:610, Leu A:570, Val A:524, Asp A:433, Leu A:479, Val A:523, Asp A:551, Ala A:521, Ile A:522, Ala A:480, Leu A:432, Val A:481, and Thr A:434. These interactions collectively contribute to the overall stability of the ligand–protein complex. The presence of both hydrogen bonding and extensive hydrophobic contacts indicates favorable binding of guggulsterone within the active site, supporting its potential inhibitory activity against the target protein.

ADMET analysis

The ADMET analysis of guggulsterone evaluated key physicochemical and pharmacokinetic parameters, including aqueous solubility, skin permeability, gastrointestinal absorption, and bioavailability. Drug-likeness assessment using Molinspiration cheminformatics confirmed that guggulsterone complies with Lipinski's rule of five, with no violations observed. The calculated molecular weight, lipophilicity (LogP), molar refractivity, hydrogen bond donors, and hydrogen bond acceptors were all within the acceptable range for orally active compounds. The corresponding numerical values are provided in Table 4 and Table 5. Gastrointestinal absorption and brain permeability were assessed using the BOILED-Egg model. As illustrated in Figure 9, guggulsterone is located within the yellow region, indicating a high probability of passive gastrointestinal absorption and predicted blood-brain barrier permeability. Collectively, these parameters indicate favorable pharmacokinetic characteristics relevant to oral drug development.

Toxicity Prediction

The toxicity prediction analysis revealed a predominantly favorable organ-specific safety profile for guggulsterone as depicted in Figure 10. The compound was predicted to be inactive for hepatotoxicity with a probability score of 0.69, indicating a low likelihood of liver-associated adverse effects. Neurotoxicity was also classified as inactive with high confidence (probability 0.97), suggesting minimal risk to the nervous system. Similarly, nephrotoxicity was predicted to be inactive (probability 0.90), reflecting a low potential for renal toxicity. Although respiratory toxicity was predicted as active, the associated high probability (0.98) indicates a minimal and context-dependent respiratory toxicity risk, which may be influenced by exposure conditions and requires experimental confirmation.

In addition, cardiotoxicity was predicted to be inactive with a probability of 0.77, suggesting a low likelihood of adverse cardiac effects. Overall, guggulsterone exhibited a largely safe toxicity profile in silico, with no major organ toxicity concerns predicted under the evaluated parameters. The toxicity predictions are summarized in Table 6 and illustrated in Figure 6.

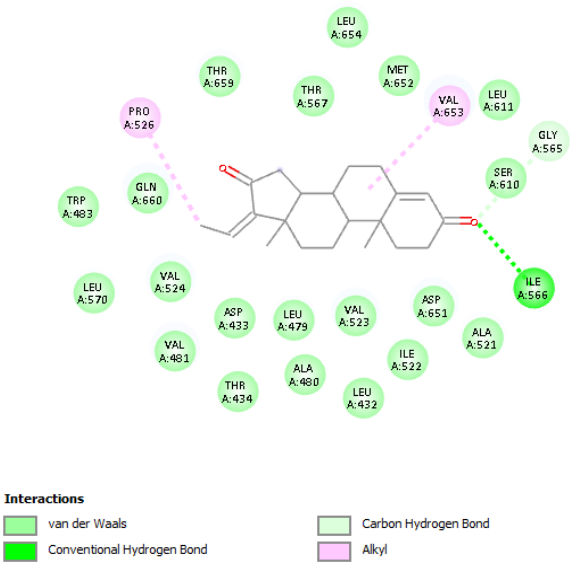

Figure 7. 2D interactions of target protein with guggulsterone

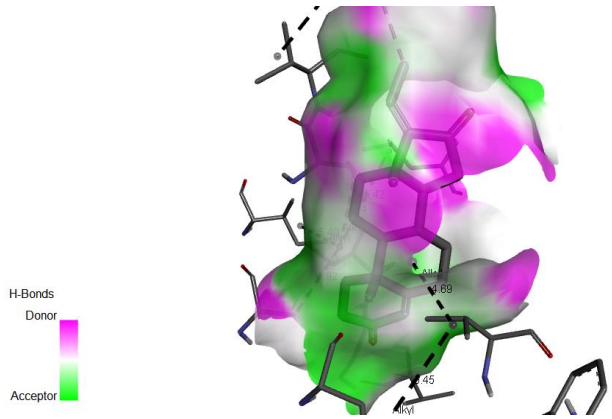

Figure 8. Hydrogen bond interaction of protein LDLR protein and guggulsterone

Table 4. ADMET parameters for Guggulsterone

ADMET Parameters	Parametric Values
Formula	$C_{21}H_{28}0_2$
Molecular weight	312.45g/mol
No. of heavy atoms	23
Fraction Csp3	0.70
No. of rotatable bonds	0
No. of Hydrogen bond acceptors	2
No. of Hydrogen bond donors	0
Molar Refractivity	93.54
Topological Polar Surface Area (TPSA)	34.14Å²
Log S (ESOL) Water solubility	-4.26
GI Absorption	High
Log Kp (Skin permeation)	-5.41cm/s
Bioavailability Score	0.55
Synthetic accessibility	4.79

Table 5. The result of Guggulsterone for Lipinski Rule of 5

Lipinski Rule of 5	Guggulsterone
Molar mass	312.45g/mol
Molar refractivity	93.54
Hydrogen bond acceptor	2
LogP	4.03
Hydrogen bond donor	0

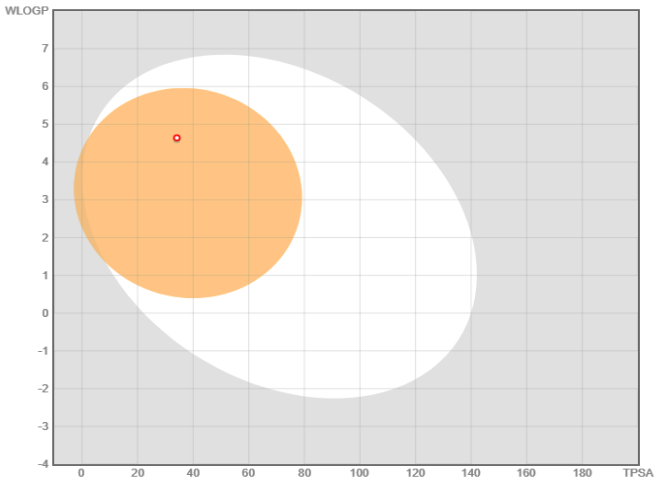

Figure 9. The boiled egg diagram for Guggulsterone, illustrates two key regions: the yellow region, representing molecules capable of assessing the blood-brain barrier, and the white region, indicating molecules absorbed in the human intestine for the predicted drug complex.

Table 6. Organ-specific toxicity prediction profile of guggulsterone showing predicted activity status and associated probability scores for hepatotoxicity, neurotoxicity, nephrotoxicity, respiratory toxicity, and cardiotoxicit.

Classification	Target	Prediction	Probability
Organ toxicity	Hepatotoxicity	Inctive	0.69
Organ toxicity	Neurotoxicity	Inctive	0.97
Organ toxicity	Nephrotoxicity	Inactive	0.90
Organ toxicity	Respiratory toxicity	Active	0.98
Organ toxicity	Cardiotoxicity	Inactive	0.77

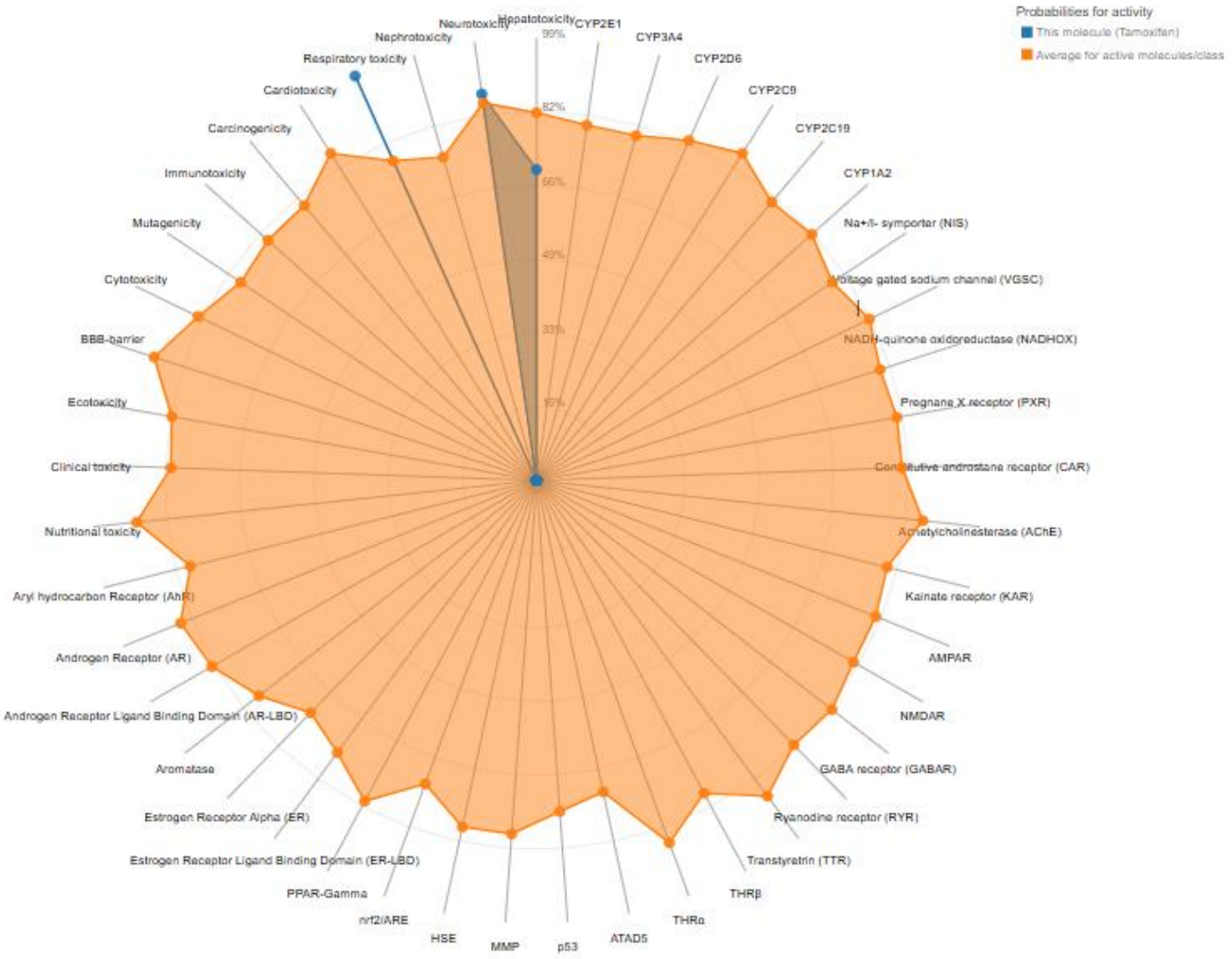

Figure 10: Guggulsterone's toxicity prediction using Pro Tox 3 involves inactive response is indicated by red dots, while active response of Guggulsterone is represented by the blue dots towards the receptor The accuracy of probability prediction increases when the yellow area on the chart graph is longer.

DISCUSSION

Familial hypercholesterolemia (FH) is an inherited disorder marked by significantly elevated low-density lipoprotein cholesterol (LDL-C), which accelerates atherosclerosis and increases the risk of premature cardiovascular disease. The majority of FH cases are caused by loss-of-function mutations in the LDLR gene, resulting in impaired LDL uptake and reduced receptor-mediated clearance. Therefore, effective therapeutic strategies aim to enhance LDLR function either by increasing receptor expression, stabilizing receptor structure, improving recycling, or preventing degradation via PCSK9 inhibition rather than inhibiting LDLR activity, which would theoretically exacerbate LDL-C accumulation. Current FH treatments, including statins, ezetimibe, PCSK9 inhibitors, and bile acid sequestrants, reflect this principle, targeting pathways that preserve or increase functional LDLR levels [18] [19] [20].

In this study, guggulsterone was identified as the most promising natural compound among five screened phytochemicals, exhibiting the highest docking affinity toward LDLR (-9.4 kcal/mol). Molecular interaction analysis revealed that guggulsterone forms a conventional hydrogen bond with ILE A:566 and hydrophobic contacts with residues

including PRO A:526 and VAL A:653, as well as multiple van der Waals interactions with surrounding amino acids. These interactions indicate a stable binding conformation within the LDLR binding pocket. While these results demonstrate strong receptor binding, the precise functional consequences of guggulsterone on LDLR activity whether it stabilizes the receptor, prevents PCSK9-mediated degradation, or affects receptor recycling remain to be experimentally validated. This distinction is critical, as any direct inhibition of LDLR would be counterproductive in FH.

Secondary structure analysis of LDLR, performed using GOR IV and PSIPRED, showed that the protein is predominantly composed of random coils (62.59%) and β-strands (28.42%), with a smaller fraction of α-helices (8.99%). PSIPRED-based topology prediction indicated that the majority of residues (1–761) reside in the extracellular domain, the transmembrane helix spans residues 762–780, and the cytoplasmic domain encompasses residues 781–834. These structural insights provide context for understanding potential ligand-binding sites and receptor modulation mechanisms. In addition, binding site prediction using DeepSite identified four distinct cavities, which may serve as regions for guggulsterone interaction and future receptor-targeted drug design.

ADMET and toxicity analyses further support the potential of guggulsterone as a drug candidate. The compound demonstrated high predicted gastrointestinal absorption, favorable drug-likeness according to Lipinski's rule of five, and low organ-specific toxicity across hepatotoxicity, neurotoxicity, nephrotoxicity, and cardiotoxicity endpoints. While blood-brain barrier permeability was predicted, this may represent a pharmacokinetic consideration rather than a therapeutic requirement, since FH is a peripheral metabolic disorder, and CNS exposure is unnecessary for efficacy.

Collectively, the results suggest that guggulsterone may serve as a natural compound capable of interacting with LDLR in a manner that could modulate receptor stability or function. However, given that FH therapy relies on enhancing LDLR activity rather than inhibition, future investigations should prioritize functional studies assessing LDLR expression, recycling, or PCSK9 interactions in the presence of guggulsterone. Experimental validation through in vitro hepatocyte models and in vivo studies is essential to determine whether the observed binding translates to clinically meaningful LDL-C lowering. This integrated computational analysis provides a foundation for further exploration of phytochemical-based approaches to FH management, emphasizing receptor modulation over inhibition.

CONCLUSION

Familial Hypercholesterolemia (FH) is a genetic disorder marked by high LDL cholesterol levels in the blood. While treatments like statins, PCSK9 inhibitors, and ezetimibe are available, they often come with significant side effects. This study explores the potential of phytochemicals, particularly guggulsterone, as a therapeutic agent targeting the LDLR protein to treat FH. In silico docking revealed guggulsterone's strong affinity for the LDLR active site. The compound was found to be non-toxic, adhere to Lipinski's rule of five, and show promising pharmacophore properties. Although these results are based on computational analysis, they suggest that plant-derived phytochemicals could be effective therapeutic candidates for FH. However, further in-vitro and in-vivo studies are needed to validate these findings.

DECLARATION

Acknowledgement

The authors express their gratitude to Gampaha Wickramarachchi University of Indigenous Medicine, Sri Lanka and Industrial Technology Institute, Sri Lanka.

Authorship contributions

Concept and Writing: Sadia Ali, Esha Shahid, Aysha Shafique, Rabia; Data Collection: Ayesha, Amad Ul Hassan, Bilal Ilyas, Zain Ul Abidin ; Computational Analysis: Tanzeel Ur Rehman, Zainab Aqsa; References and Citations: Ayesha Nawaz; Manuscript Drafting and Editing: Areeba Younas, Maham Rafique

Funding

The present research received no grant from any funding agency.

Ethics approval and consent to participate

This research was conducted entirely using in silico approaches and publicly available databases. No experiments involving human participants or animals were performed; therefore, ethical approval and informed consent were not required.

Competing interests

The authors declared that there is no conflict of interest.

REFERENCES

Benito-Vicente, A., Uribe, K. B., Jebari, S., Galicia-Garcia, U., Ostolaza, H., Martin, C. (2018). Familial hypercholesterolemia: the most frequent cholesterol metabolism disorder caused disease. International Journal of Molecular Sciences 19:3426. https://doi.org/10.3390/ijms19113426

Foody, J. M., Vishwanath, R. (2016). Familial hypercholesterolemia/autosomal dominant hypercholesterolemia: molecular defects, the LDL-C continuum, and gradients of phenotypic severity. Journal of Clinical Lipidology 10:970–986. https://doi.org/10.1016/j.jacl.2016.04.009

Di Taranto, M. D., Fortunato, G. (2023). Genetic heterogeneity of familial hypercholesterolemia: repercussions for molecular diagnosis. International Journal of Molecular Sciences 24:3224. https://doi.org/10.3390/ijms24043224

Rogozik, J., Główczyńska, R., Grabowski, M. (2024). Genetic backgrounds and diagnosis of familial hypercholesterolemia. Clinical Genetics 105:3–12. https://doi.org/10.1111/cge.14435

Suryawanshi, Y. N., Warbhe, R. A. (2023). Familial hypercholesterolemia: a literature review of the pathophysiology and current and novel treatments. Cereus. https://doi.org/10.7759/cureus.49121

Hanif, N., Arif, A. A. A., Ali, S. A. S., Anees, M. A. M., Anees, M. A. M., Arshad, A., Asim, M. (2025). Computational drug design targeting MYH7 for hypertrophic cardiomyopathy integrating molecular docking, Density Functional Theory, and Molecular Dynamics Simulations. Journal of Applied Biological Sciences 19:179–192. https://doi.org/10.71336/jabs.1477

Naveed, M., Ali, N., Aziz, T., Hanif, N., Fatima, M., Ali, I., Albekairi, T. H. (2024). The natural breakthrough: phytochemicals as potent therapeutic agents against spinocerebellar ataxia type 3. Scientific Reports 14:1529. https://doi.org/10.1038/s41598-024-51954-3

Naveed, M., Hussain, M., Aziz, T., Hanif, N., Kanwal, N., Arshad, A., Alharbi, M. (2024). Computational biology assisted exploration of phytochemicals derived natural inhibitors to block BZLF1 gene activation of Epstein–Bar virus in host. Scientific Reports 14:31664. https://doi.org/10.1038/s41598-024-81037-2

Hussain, M., Kanwal, N., Jahangir, A., Ali, N., Hanif, N., Ullah, O. (2024). Computational modeling of cyclotides as antimicrobial agents against Neisseria gonorrhoeae PorB porin protein: integration of docking, immune, and molecular dynamics simulations. Frontiers in Chemistry 12:1493165. https://doi.org/10.3389/fchem.2024.1493165

Crosara, K. T. B., Moffa, E. B., Xiao, Y., Siqueira, W. L. (2018). Merging in-silico and in vitro salivary protein complex partners using the STRING database: a tutorial. Journal of Proteomics 171:87–94. https://doi.org/10.1016/j.jprot.2017.08.002

Zhang, Y., Qiao, S., Ji, S., Li, Y. (2020). DeepSite: bidirectional LSTM and CNN models for predicting DNA–protein binding. International Journal of Machine Learning and Cybernetics 11:841–851. https://doi.org/10.1007/s13042-019-00990-x

Naveed, M., Hanif, N., Aziz, T., Waseem, M., Alharbi, M., Alshammari, A., Alasmari, A. F. (2025). Insight into molecular and mutational scrutiny of epilepsy associated gene Gabrg2 leading to novel computer-aided drug designing. Scientific Reports 15:6770. https://doi.org/10.1038/s41598-025-91505-y

Faizan, R., Naveed, M., Estevez, I. B., Hanif, N., Arshad, A., Aziz, T., Alhomrani, M. (2025). Computational exploration of natural inhibitors against toxin-associated proteins in Naegleria fowleri Karachi strain. Pathology-Research and Practice 221:156184. https://doi.org/10.1016/j.prp.2025.156184

Liu, Y., Cao, Y. (2023). Protein–Ligand Blind Docking Using CB-Dock2. In: Computational Drug Discovery and Design. New York, NY: Springer US, pp. 113–125. https://doi.org/10.1007/978-1-0716-3441-7_6

Temml, V., Kaserer, T., Kutil, Z., Landa, P., Vanek, T., Schuster, D. (2014). Pharmacophore modeling for COX-1 and -2 inhibitors with LigandScout in comparison to Discovery Studio. Future Medicinal Chemistry 6:1869–1881. https://doi.org/10.4155/fmc.14.114

Rauf, A., Khan, H., Khan, M., Abusharha, A., Serdaroğlu, G., Daglia, M. (2023). In silico, SwissADME, and DFT studies of newly synthesized oxindole derivatives followed by antioxidant studies. Journal of Chemistry 2023:5553913. https://doi.org/10.1088/1755-1315/890/1/012021

Banerjee, P., Ulker, O. C. (2022). Combinative ex vivo studies and in silico models ProTox-II for investigating the toxicity of chemicals used mainly in cosmetic products. Toxicology Mechanisms and Methods 32:542–548. https://doi.org/10.1080/15376516.2022.2053623

McGowan, M. P., Hosseini Dehkordi, S. H., Moriarty, P. M., Duell, P. B. (2019). Diagnosis and treatment of heterozygous familial hypercholesterolemia. Journal of the American Heart Association 8:e013225. https://doi.org/10.1161/JAHA.119.01322

Vuorio, A., Watts, G. F., Schneider, W. J., Tsimikas, S., Kovanen, P. T. (2020). Familial hypercholesterolemia and elevated lipoprotein (a): double heritable risk and new therapeutic opportunities. Journal of Internal Medicine 287:2–18. https://doi.org/10.1111/joim.12981

Reiner, Ž. (2015). Management of patients with familial hypercholesterolaemia. Nature Reviews Cardiology 12:565–575. https://doi.org/10.1038/nrcardio.2015.92

Publisher's note: Anatolia Academy of Sciences Ltd. remains neutral with regard to jurisdictional claims in published maps and institutional affiliations.

Open Access: This article is licensed under a Creative Commons Attribution 4.0 International License, which permits use, sharing, adaptation, distribution and reproduction in any medium or format, as long as you give appropriate credit to the original author(s) and the source, provide a link to the Creative Commons licence, and indicate if changes were made. The images or other third party material in this article are included in the article's Creative Commons licence, unless indicated otherwise in a credit line to the material. If material is not included in the article's Creative Commons licence and your intended use is not permitted by statutory regulation or exceeds the permitted use, you will need to obtain permission directly from the copyright holder. To view a copy of this licence, visit https://creativecommons.org/licenses/by/4.0/.

© The Author(s) 2026